Cell Reports

Report

# Platinum and PARP Inhibitor Resistance Due to Overexpression of MicroRNA-622 in *BRCA1*-Mutant Ovarian Cancer

## Graphical Abstract

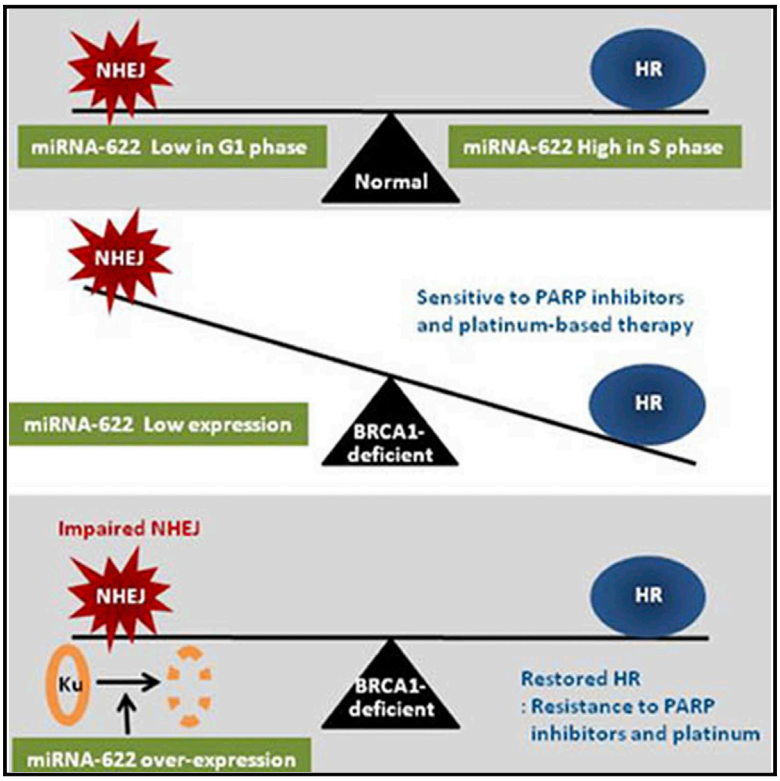


## Highlights

- miR-622 induces resistance to PARP inhibitors and cisplatin in *BRCA1*-deficient cells
- miR-622 levels in *BRCA1*-mutant ovarian tumors correlates with survival of patients
- The Ku complex is directly downregulated by miR-622 to suppress the NHEJ pathway
- MiR-622 helps to balance HR and NHEJ pathways for DSB repair during the cell cycle

## Authors

Young Eun Choi, Khyati Meghani, Marie-Eve Brault, ..., Douglas A. Levine, Panagiotis A. Konstantinopoulos, Dipanjan Chowdhury

## Correspondence

panagiotis_konstantinopoulos@dfci.harvard.edu (P.A.K.), dipanjan_chowdhury@dfci.harvard.edu (D.C.)

## In Brief

Choi et al. show that expression of miR-622 induces resistance to PARP inhibitors and cisplatin in *BRCA1*-mutant ovarian tumors and correlates with survival of patients. miR-622 suppresses NHEJ by downregulating expression of the Ku complex and facilitates homologous recombination mediated repair of DNA double-strand breaks (DSBs) in the S phase of cycling cells.

Choi et al., 2016, Cell Reports *14*, 1–11
January 26, 2016 ©2016 The Authors
http://dx.doi.org/10.1016/j.celrep.2015.12.046

CellPress

Please cite this article in press as: Choi et al., Platinum and PARP Inhibitor Resistance Due to Overexpression of MicroRNA-622 in *BRCA1*-Mutant Ovarian Cancer, Cell Reports (2016), http://dx.doi.org/10.1016/j.celrep.2015.12.046

Cell Reports
Report

OPEN ACCESS
CellPress

# Platinum and PARP Inhibitor Resistance Due to Overexpression of MicroRNA-622 in *BRCA1*-Mutant Ovarian Cancer

Young Eun Choi,[1] Khyati Meghani,[1] Marie-Eve Brault,[1] Lucas Leclerc,[1] Yizhou J. He,[1] Tovah A. Day,[2] Kevin M. Elias,[3] Ronny Drapkin,[4] David M. Weinstock,[2] Fanny Dao,[5] Karin K. Shih,[5] Ursula Matulonis,[2] Douglas A. Levine,[5] Panagiotis A. Konstantinopoulos,[2,*] and Dipanjan Chowdhury[1,*]
[1]Division of Genomic Stability and DNA Repair, Department of Radiation Oncology
[2]Department of Medical Oncology
Dana-Farber Cancer Institute, Harvard Medical School, Boston, MA 02215, USA
[3]Division of Gynecologic Oncology, Department of Obstetrics and Gynecology and Reproductive Biology, Brigham and Women's Hospital, Boston, MA 02215, USA
[4]Ovarian Cancer Research Center, Department of Obstetrics and Gynecology, University of Pennsylvania, Perelman School of Medicine, Philadelphia, PA 19104, USA
[5]Department of Surgery, Memorial Sloan Kettering Cancer Center, Weill Cornell Medical College, New York, NY 10065, USA
*Correspondence: panagiotis_konstantinopoulos@dfci.harvard.edu (P.A.K.), dipanjan_chowdhury@dfci.harvard.edu (D.C.)
http://dx.doi.org/10.1016/j.celrep.2015.12.046
This is an open access article under the CC BY-NC-ND license (http://creativecommons.org/licenses/by-nc-nd/4.0/).

## SUMMARY

**High-grade serous ovarian carcinomas (HGSOCs) with *BRCA1/2* mutations exhibit improved outcome and sensitivity to double-strand DNA break (DSB)-inducing agents (i.e., platinum and poly(ADP-ribose) polymerase inhibitors [PARPis]) due to an underlying defect in homologous recombination (HR). However, resistance to platinum and PARPis represents a significant barrier to the long-term survival of these patients. Although *BRCA1/2*-reversion mutations are a clinically validated resistance mechanism, they account for less than half of platinum-resistant *BRCA1/2*-mutated HGSOCs. We uncover a resistance mechanism by which a microRNA, miR-622, induces resistance to PARPis and platinum in *BRCA1* mutant HGSOCs by targeting the Ku complex and restoring HR-mediated DSB repair. Physiologically, miR-622 inversely correlates with Ku expression during the cell cycle, suppressing non-homologous end-joining and facilitating HR-mediated DSB repair in S phase. Importantly, high expression of miR-622 in *BRCA1*-deficient HGSOCs is associated with worse outcome after platinum chemotherapy, indicating microRNA-mediated resistance through HR rescue.**

## INTRODUCTION

Approximately 15%–20% of patients with epithelial ovarian cancer (EOC) harbor germline (10%–15%) or somatic (6%–7%) *BRCA1* or *BRCA2* mutations (TCGA, 2011). Furthermore, epigenetic silencing *of BRCA1* via promoter hypermethylation occurs in ~10%–20% of EOCs. Due to the underlying defect in DNA repair via homologous recombination (HR), patients with *BRCA1/2*-inactivated EOCs exhibit enhanced sensitivity to platinum analogs and other cytotoxic drugs that induce double-strand DNA breaks (DSBs) such as the poly(ADP ribose) polymerase inhibitors (PARPis) (Fong et al., 2009). Of these drugs, olaparib was granted accelerated approval by the US Food and Drug Administration for use in EOC patients with germline *BRCA1/2* mutations (Fong et al., 2009). However, a substantial fraction of these patients do not respond or eventually develop resistance to these agents, suggesting that de novo and acquired platinum and PARPi resistance is a significant clinical problem in HR-defective EOCs. The most common mechanism of resistance to these agents in *BRCA1/2*-mutated tumors is secondary intragenic mutations restoring BRCA1 or BRCA2 protein functionality; 46% of platinum-resistant *BRCA*-mutated EOCs exhibit tumor-specific secondary mutations that restore the open reading frame of either *BRCA1* or *BRCA2* (Norquist et al., 2011).

The interplay of the two major mechanistically distinct DSB repair pathways, HR and non-homologous end-joining (NHEJ) (Chapman et al., 2012b; Ciccia and Elledge, 2010), is also critical for resistance to platinum and PARPis. Surprisingly, the sensitivity of *BRCA1*-mutant tumors to PARPis is almost completely abolished by loss of the NHEJ factor 53BP1 (Bouwman et al., 2010; Bunting et al., 2010; Chapman et al., 2012a), which also correlates with the restoration of competent HR. Furthermore, a recent small hairpin RNA (shRNA) screen for hairpins promoting survival of *BRCA1*-deficient mouse mammary tumors to PARPis identified 53BP1 and REV7, a factor implicated in NHEJ, as the top hits (Boersma et al., 2015; Xu et al., 2015). However, unlike *BRCA1/2* reversion mutations, these resistance mechanisms have not been shown to be clinically relevant for patients with *BRCA1/2*-inactivated EOCs. However, it is feasible that the NHEJ pathway may be relevant for PARPi resistance in

EOCs, and other NHEJ factors may contribute to the resistant phenotype.

Here, we uncover mechanism of resistance to PARPi and platinum in *BRCA1*-mutated EOCs that involves microRNA (miRNA)-mediated regulation of NHEJ. Specifically, we have identified a miRNA, miR-622, that regulates the expression of the Ku-complex and specifically suppresses NHEJ during S-phase. Consistent with this effect, overexpression of miR-622 rescues the HR-deficiency of *BRCA1* mutant ovarian tumor lines and induces resistance to PARPi and platinum-based drugs. Furthermore, expression of miR-622 in two cohorts of patients with *BRCA1*-inactivated EOCs correlates with reduced disease-free survival after platinum-based therapy, suggesting direct clinical relevance in patients with EOC.

## RESULTS

### miR-622 "Desensitizes" *BRCA1*-Mutant Cells to PARP Inhibitors and Platinum-Based Therapy

Recently, we used PARPi sensitivity as a marker for HR deficiency to conduct a functional screen for identifying miRNAs that downregulate HR in a breast cancer line, MDA-MB231 (Choi et al., 2014). We characterized the miRNAs (miR-1255b, miR-193b*, and miR-148b*) that suppress HR by downregulating the expression of *BRCA1*, *BRCA2*, and *RAD51*. Strikingly, in that screen, six miRNAs (miR-644, miR-492, miR-613, miR-577, miR-622, and miR-126*) (Choi et al., 2014) demonstrated a surprising trend of inducing PARPi resistance. Our original screen was conducted to assess the impact of these miRNAs on PARPi sensitivity in a *BRCA* proficient breast cancer line MDA-MB231. Considering *BRCA*-mutant cells are responsive to PARPi, we also examined the impact of these miRNAs in a *BRCA1*-mutant breast line, MDA-MB436. There was no significant impact of miR-644, miR-492, miR-613, miR-577, and miR-126* on PARPi sensitivity in MDA-MB231 and MDA-MB436 cells (Figure S1A); however, miR-622 significantly induced resistance to the clinical-grade PARPis olaparib and veliparib specifically in the MDA-MB436 cells (Figure S1B). Furthermore, we tested the impact of miR-622 on PARPi sensitivity on the *BRCA1*-mutant EOC line UWB1.289 and found that overexpression of miR-622 caused resistance to both PARPis, olaparib and veliparib (ABT-888) (Figure 1A). Interestingly, miR-622 expression also caused resistance to the platinum-based chemotherapeutic agents carboplatin and cisplatin in the *BRCA1*-mutated UWB1.289 cells (Figure 1A). Importantly, restoring *BRCA1* expression in UWB1.289 cells completely negates the impact of miR-622 on PARPi sensitivity and also sensitivity to platinum drugs (Figure S1C). In order to exclude the possibility that the *Brca1*-mutant lines MDA-MB436 and UWB1.289 have acquired other unaccounted mutations that may contribute to the phenotype induced by miR-622, we expressed miR-622 in *BRCA1* null mouse embryonic fibroblasts (MEFs) and assessed sensitivity to olaparib and cisplatin. Consistent with our previous results, miR-622 significantly "desensitized" *Brca1*$^{-/-}$ MEFs to both drugs (Figure 1B) but did not impact the sensitivity of their wild-type counterparts (Figure S1D). Together, these data suggest that the impact of miR-622 on PARPi- and platinum-based therapy is specific to the loss of *BRCA1*.

### Expression of miR-622 Correlates with Response to Platinum Chemotherapy in *BRCA1*-Inactivated EOCs

To evaluate the association between miR-622 expression and platinum response in EOCs with *BRCA1* inactivation, we assessed data from the ovarian TCGA dataset (TCGA, 2011). In that dataset, 89 EOCs (all high-grade serous ovarian carcinomas [HGSOCs]) exhibited *BRCA1*-inactivation; 38 EOCs harbored *BRCA1* mutations (out of 316 EOCs that underwent whole-exome sequencing), while 51 tumors (out of 489 tumors with DNA promoter methylation data) harbored *BRCA1* epigenetic silencing via promoter hypermethylation. All patients underwent surgery followed by platinum-based chemotherapy. We evaluated the association between miR-622 expression and platinum response using various cutoffs for low versus high miR-622 expression. In all cases, we consistently found that tumors with higher miR-622 expression were associated with inferior response to first-line platinum-based chemotherapy and worse survival. Specifically, using median miR-622 expression as a threshold to classify *BRCA1*-inactivated EOCs as exhibiting high versus low miR-622 expression, we found that *BRCA1*-inactivated tumors with high expression of miR-622 were associated with worse disease-free survival (DFS) (median DFS 14.7 versus 19.8 months, respectively, log rank $p = 0.03$) and overall survival (OS) (median OS 39 versus 49.3 months, respectively, log rank $p = 0.03$) compared with tumors with low miR-622 expression (Figure 1C). Conversely, there was no association between miR-622 expression and outcome, DFS, or OS in the remaining tumors in the TCGA dataset, i.e., those without *BRCA1* mutations and without *BRCA1* promoter hypermethylation (data not shown). This trend was particularly evident in tumors with the highest miR-622 expression, i.e., those whose miR-622 expression was in the highest quintile. Specifically, *BRCA1*-inactivated tumors whose expression levels for miR-622 were in the highest quintile were associated with worse DFS (median DFS 13.7 versus 18.1 months, respectively, log rank $p = 0.005$) and OS (median OS 35.3 versus 48.3 months, respectively, log rank $p = 0.001$; Figure 1D).

Furthermore, we compared tumors with the highest miR-622 expression versus those with the lowest miR-622 expression. Specifically, when comparing the top 5, 10, or 15 tumors with the highest miR-622 expression with the lowest 5, 10, or 15 tumors, respectively, we consistently found that the tumors with the highest miR-622 expression were associated with inferior response to first-line platinum chemotherapy, i.e., worse DFS and OS compared to the tumors with the lowest expression (Figures 1E and S1E).

Given the absence of other miRNA expression datasets with sizeable numbers of ovarian tumors with *BRCA1*-mutations or *BRCA1* promoter hypermethylation, we explored the correlation between miR-622 and outcome in tumors with low *BRCA1* expression in a different, clinically annotated ovarian cancer dataset (Shih et al., 2011). This dataset included miRNA and mRNA expression data from 60 patients with newly diagnosed FIGO stage III or IV tumors with serous histology, including 3 tumors with *BRCA1* mutations. As shown in Figure S1F, we found similar correlation between high miR-622 expression and inferior outcome to first line platinum based chemotherapy.

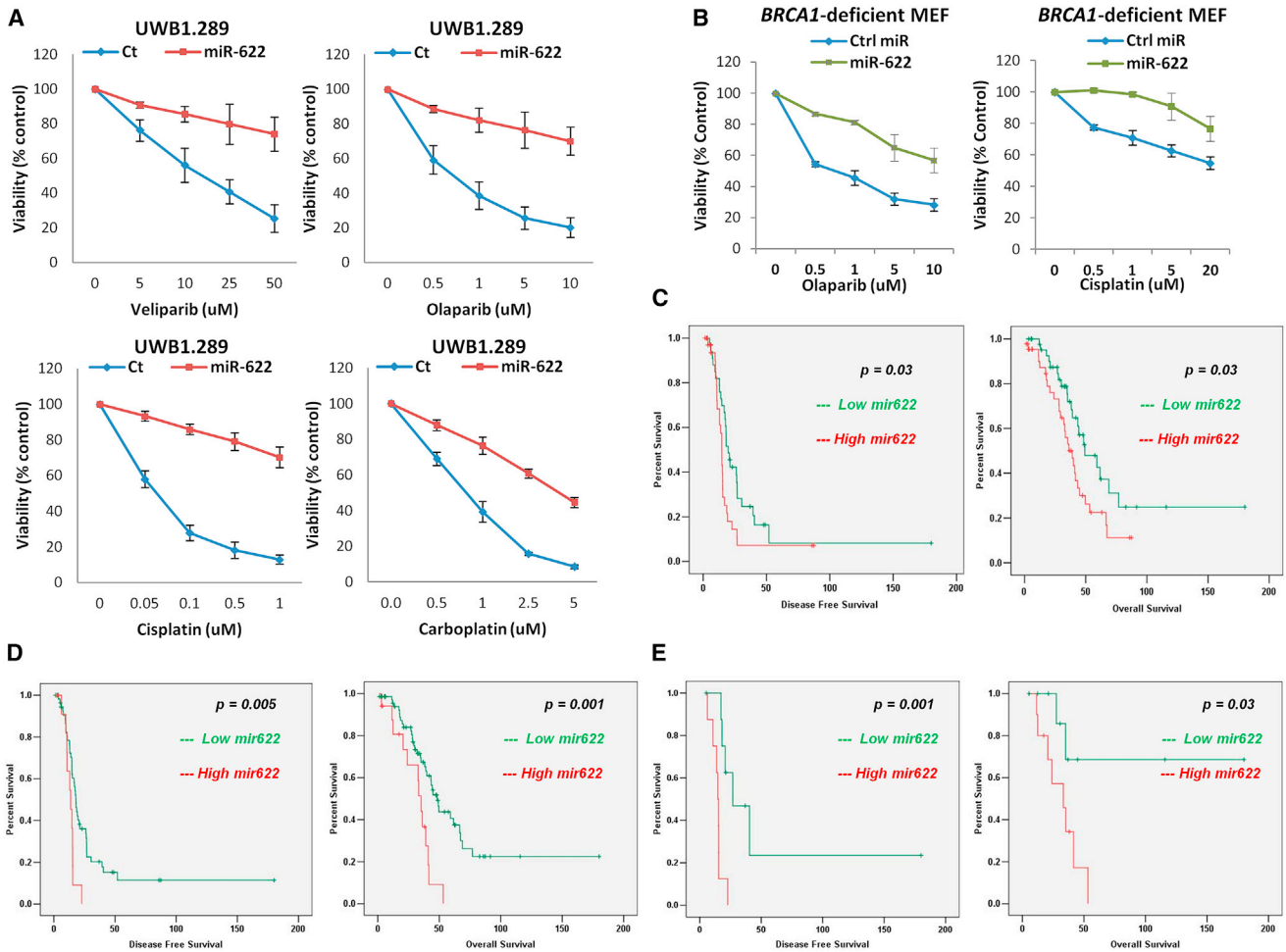


**Figure 1. miRNA-Mediated Resistance to PARP Inhibitors and Platinum in *BRCA1* Mutant Cells**

(A and B) Viability assays to examine the impact of miR-622 on drug sensitivity. *BRCA1* null UWB1.289 cells (A) or *Brca1*-deficient MEF cells (B) were transfected with control mimic or miR-622 mimic and treated with vehicle or indicated drug before measurement of viability by luminescence-based ATP quantification. Curves were generated from three independent experiments.

(C) Association between miR-622 expression levels and DFS and OS in tumors with *BRCA1* mutation and *BRCA1* promoter hypermethylation in the TCGA dataset based on 50% cutoff. Tumors with *BRCA1* mutations and *BRCA1* promoter hypermethylation with above-median expression levels of miR-622 were associated with worse DFS (left, log rank p = 0.03) and OS (right, log rank p = 0.03).

(D) Association between miR-622 expression levels and DFS and OS in tumors with *BRCA1* mutation and *BRCA1* promoter hypermethylation in the TCGA dataset based on 20% cutoff. Tumors with *BRCA1* mutations and *BRCA1* promoter hypermethylation whose expression levels for miR-622 were in the highest quintile were associated with worse DFS (left, log rank p = 0.005) and OS (right, log rank p = 0.001).

(E) DFS and OS in the ten tumors with the highest miR-622 expression versus the ten tumors with the lowest miR-622 expression in the TCGA dataset (tumors with *BRCA1* mutation and *BRCA1* promoter hypermethylation). The ten tumors with the lowest miR-622 expression were associated with worse DFS (left, log rank p = 0.001) and OS (right, log rank p = 0.03) compared to the ten tumors with the highest miR-622 expression.

## miR-622 Impacts NHEJ-Mediated Repair of DSBs

The NHEJ pathway is composed of at least two branches: the well-studied classical NHEJ (C-NHEJ) and the poorly understood alternative end-joining (A-NHEJ) (Deriano and Roth, 2013). The molecular details and biological function of A-NHEJ remains largely unclear (Deriano and Roth, 2013). Loss or depletion of factors promoting C-NHEJ (such as 53BP1) or essential for C-NHEJ (such as Ku70) induces PARPi resistance in *BRCA1*-deficient mouse cells (Bunting et al., 2010, 2012). To test whether miR-622 indeed impacts NHEJ, we assayed for C-NHEJ- and A-NHEJ-mediated repair of the yeast endonuclease, I-SceI-induced DSBs, using the EJ5-GFP reporter and EJ2-GFP reporter, respectively. These are integrated fluorescence-based reporters (Bennardo et al., 2008) that allow for efficient quantification of the two distinct NHEJ pathways at targeted DSBs. We observed that miR-622 significantly impedes C-NHEJ (Figure 2A) and enhances A-NHEJ (Figure 2B). This is consistent with studies showing that depletion of C-NHEJ factors increases the frequency of A-NHEJ (Fattah et al., 2010). Depletion of 53BP1 and Ku70 induces PARPi resistance in *BRCA1*-mutant cells by restoring HR-mediated repair of DSBs and significantly enhancing genomic stability

OPEN ACCESS
CellPress

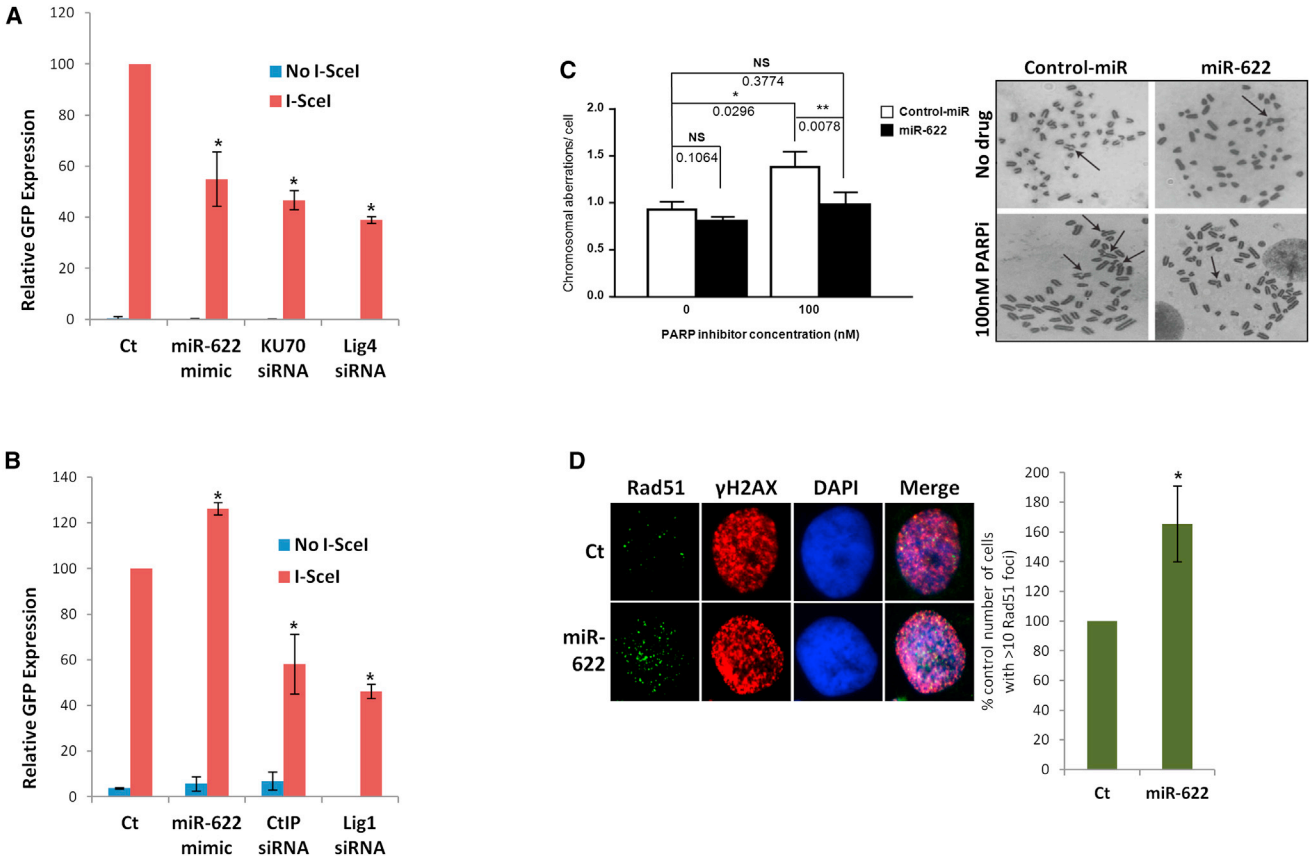


**Figure 2. Impact of miR-622 on Genome Stability and NHEJ Repair Pathways**

(A and B) Measurement of C-NHEJ-mediated (A) or A-NHEJ-mediated (B) repair of I-SceI-induced site-specific DSBs. Cells carrying a single copy of the recombination substrate with two tandem I-SceI sites were transfected with control mimic, miR-622 mimic, Ku70 small interfering RNA (siRNA), or Ligase4 siRNA before transfection with I-SceI or control vector. After 48 hr, GFP-positive cells were analyzed by flow cytometry.

(C) Analysis of genomic instability in metaphase. *Brca1*$^{-/-}$ MEF cells were transfected with control miRNA mimic or miR-622, treated with 100nM PARP inhibitor, and measured for abnormal chromosomes in metaphase ($n \geq 50$ metaphases).

(D) Analysis of HR-mediated repair by RAD51 focus formation. UWB1.289 cells were transfected with control miRNA mimic or miR-622 and stained for RAD51 (green), γH2AX (red), and 4′,6-diamidino-2-phenylindole (DAPI) (blue) 6 hr after exposure to 10Gy IR. The images were captured by fluorescence microscopy and RAD51 focus-positive cells (with >20 foci) were quantified by comparing 100 cells.

after PARPi treatment (Bunting et al., 2010, 2012). Consistent with its impact on NHEJ, we observe that expression of miR-622 in *Brca1*$^{-/-}$ MEFs causes a significant decrease in the level of genomic instability (chromosomal aberrations) induced by olaparib treatment (Figure 2C). To address the mechanism by which miR-622 promotes genome integrity in *BRCA1* mutant cells, we tested whether its expression could cause an increase in irradiation-induced Rad51 foci, a measure of the HR pathway. We found that expression of miR-622 in UWB1.289 cells caused a statistically significant increase in Rad51 foci (Figure 2D). Importantly, none of these effects are due to alterations in the cell cycle caused by the miR-622 mimics (Figure S2A).

## miR-622 Regulates Expression of the Ku Complex

To investigate the mechanism by which miR-622 influences NHEJ and impacts PARPi sensitivity, we used a candidate-based approach whereby all genes implicated in NHEJ were screened for miRNA recognition elements (MREs) of miR-622 using the PITA algorithm. This algorithm is unique in allowing G:U wobbles or seed mismatches and identifies base pairing beyond the 5′ end of the miRNA, predicts the sites not restricted to the 3′UTR of mRNA, and identifies non-canonical MREs for specific miRNA/mRNA combinations (Lal et al., 2009). Using this algorithm, miR-622 was predicted to target the transcripts of 53BP1, Ku70, Ku80, APTX, and APLF (Figure S3). We assessed the impact of overexpressing miR-622 in UWB1.289 cells on the mRNA level of these genes and observed a significant reduction in the transcripts of 53BP1, Ku70, and Ku80 (Figure 3A). Subsequently, we determined the impact of miR-622 on the protein level of their putative targets. Overexpressing miR-622 reduces the protein levels of Ku70 and Ku80 in UWB1.289 cells. The basal expression of the Ku proteins is lower in MEFs, and the impact of miR-622 on Ku70 and Ku80 in *Brca1*$^{-/-}$ MEFs is even more pronounced (Figure 3B). On the contrary, there was no detectable impact of miR-622 on

OPEN ACCESS
CellPress

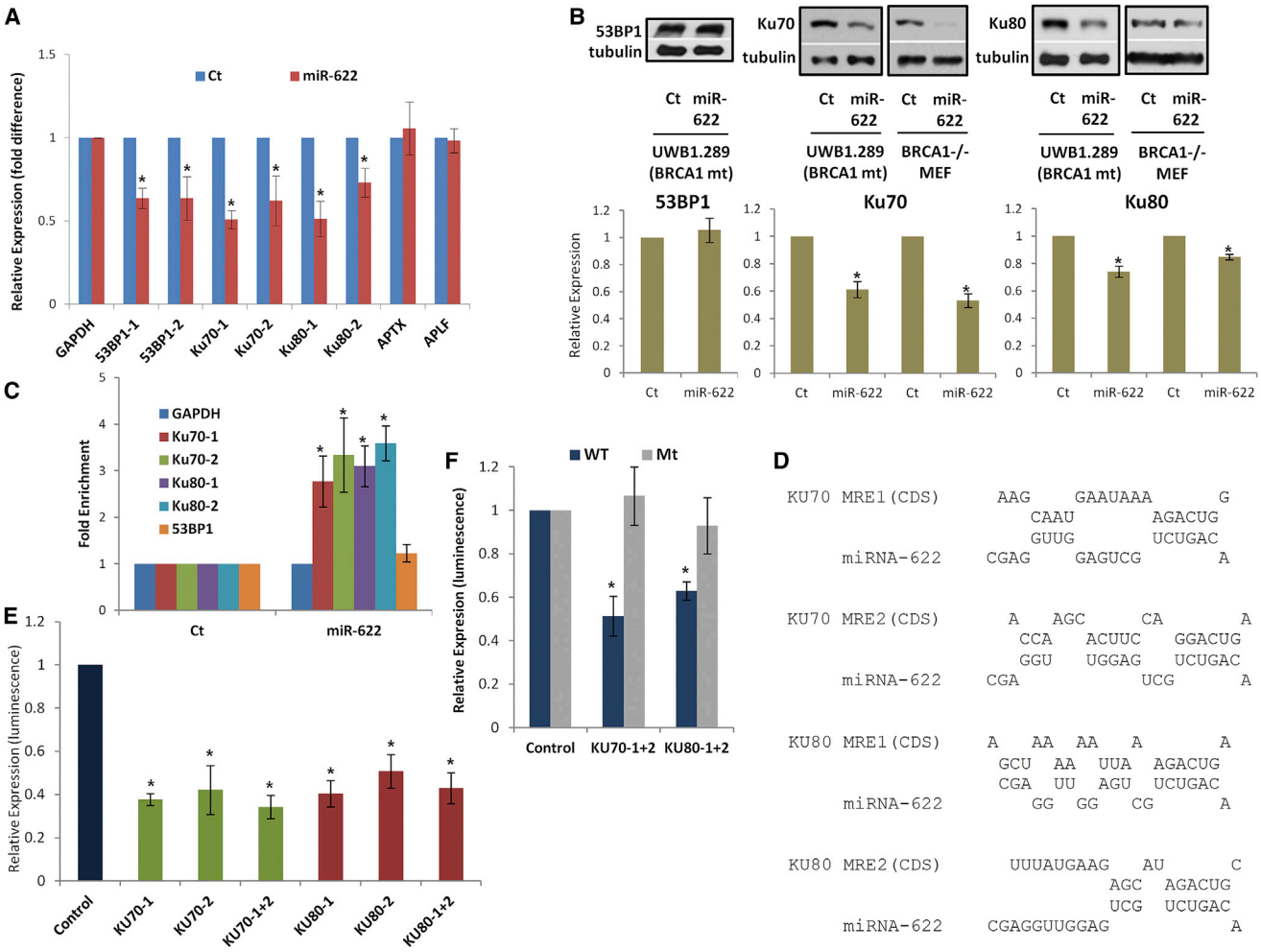


**Figure 3. Identifying and Validating Targets of miR-622**

(A and B) Expression of DNA damage response (DDR) genes is impacted by miR-622. UWB1.289 cells were transfected with control mimic or miR-622 mimic and mRNA levels of predicted DDR genes were analyzed by real-time qPCR using gene-specific primers and normalized to GAPDH (A). Cell lysates were then analyzed by immunoblot for factors that had statistically significant reduction in mRNA in cells transfected with miR-622 (B). Images were quantified by ImageJ software and the mean ± SD of three independent experiments is graphically shown.

(C) Interaction of target transcripts with miR-622. UWB1.289 cells were transfected with biotinylated-control mimic or biotinylated miR-622 mimic. The immunoprecipitated RNA was analyzed by real-time qPCR using gene-specific primers and normalized to GAPDH.

(D) Predicted MREs were obtained from PITA algorithm (http://genie.weizmann.ac.il/pubs/mir07/mir07_prediction.html) and their mutants were generated by mutating nucleotides providing complementarity to miR-622. CDS (coding sequence) means the region in the gene where the MRE is located.

(E) Luciferase reporter assay to assess direct interaction of miR-622 with target genes. Individual or combinations of predicted miRNA recognition sites (MREs) for each putative target transcript of miR-622 were cloned into the luciferase reporter vector and transfected in UWB1.289 cells along with miRNA mimics. *Renilla* luciferase activity of the reporter was measured 48 hr after transfection by normalization to an internal *firefly* luciferase control.

(F) Luciferase reporter assay for wild-type or mutant MREs for miRNA-622 targets was performed as described in Figure 2I.

Mean ± SD of three independent experiments is shown and statistical significance is indicated by $^*p < 0.05$.

53BP1 protein levels in the UWB1.289 cells. To test for association of miR-622 with the Ku70 and Ku80 transcripts, we captured miRNA-mRNA complexes using streptavidin-coated beads from cells transfected with biotinylated forms of the miRNA mimic (Lal et al., 2011; Orom and Lund, 2007). The amount of Ku70, Ku80, and 53BP1 transcripts was measured in the pull-downs, and the enrichment was assessed relative to pull-down with biotinylated control mimic and also with GAPDH. Consistent with our previous results, miR-622 selectively pulled down Ku70 and Ku80 transcripts, but not the 53BP1 transcript (Figure 3C). To verify further that Ku70 and Ku80 are targets of miR-622 and confirm that the interaction is mediated by the predicted MREs, we used luciferase reporter assays. The predicted MREs (Figure 3D) were cloned in the 3′ UTR of the luciferase gene, and expression monitored in cells transfected with the miR-622 mimic (Figure 3E). As anticipated, there was significant decrease in luciferase activity, and this was "rescued" by point mutations that disrupt base pairing between miR-622 and their corresponding

OPEN ACCESS
CellPress

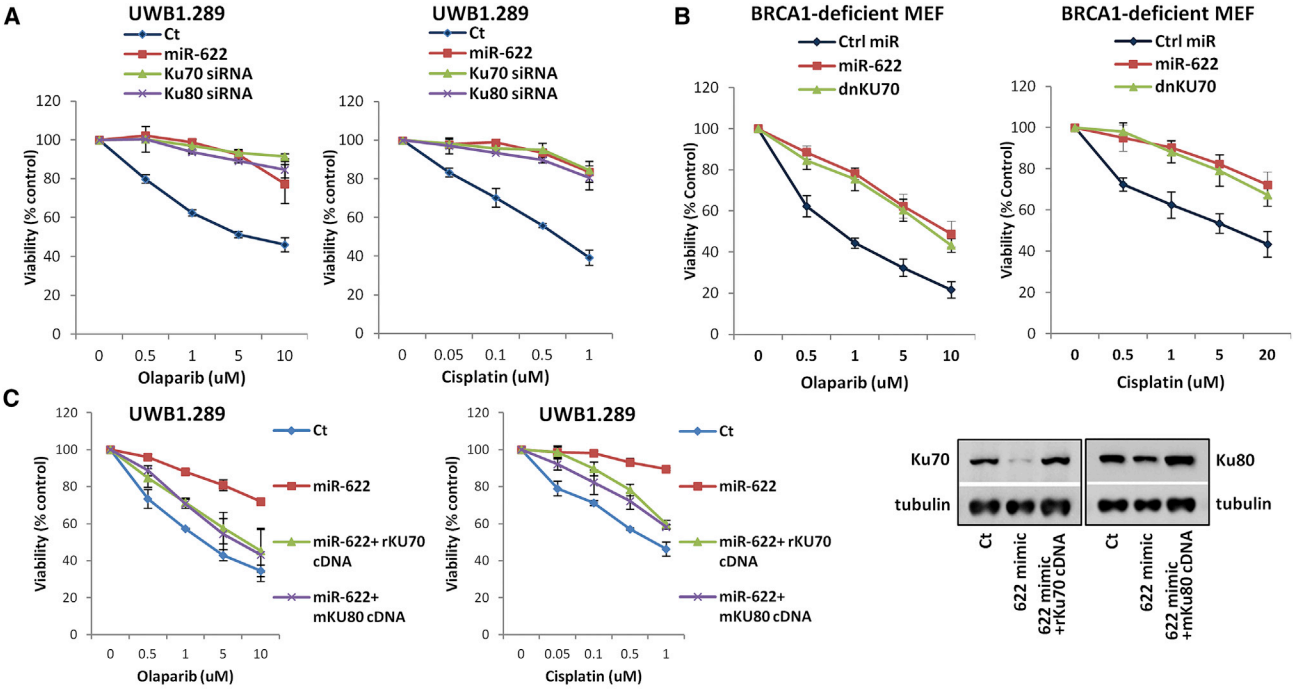


D

| Relationship | Pearson Correlation | Covariance | P value (two sided) |
|---|---|---|---|
| miR622 expression levels / Ku80 RNA expression levels | -0.249 | -0.354 | 0.019 |
| miR622 expression levels / Ku80 protein levels (RPPA) | -0.273 | -0.322 | 0.029 |

E

| Relationship | Pearson Correlation | Covariance | P value (two sided) |
|---|---|---|---|
| miR622 expression levels / Ku80 RNA expression levels | -0.255 | -0.24 | 0.05 |

**Figure 4. Correlating the Impact of miR-622 and Its Target, the Ku Complex**

(A and B) Viability assays to examine the impact of miR-622 on targets. Control mimic, miR-622 mimic, Ku70 siRNA, Ku80 siRNA, or dominant-negative Ku70 was introduced to UWB1.289 cells (A) or *BRCA1*-deficient MEF cells (B). Transfected cells were treated with vehicle or the indicated drug before viability measurement as explained in Figure 1.

(C) Impact of miRNA target rescue. UWB1.289 cells were transfected with control mimic or miR-622 mimic with or without rat Ku70 cDNA or mouse Ku80 cDNA and treated with vehicle or the indicated drug before viability measurement as explained in Figure 1. Expression of introduced genes was examined by immunoblot.

(D) Correlation among miR-622 expression levels, Ku80 RNA expression levels, and Ku80 protein levels in the TCGA dataset. miR-622 expression levels were statistically significantly inversely correlated with Ku80 RNA expression levels ($p = 0.019$) and Ku80 protein levels ($p = 0.029$).

(E) Correlation between miR-622 expression levels and Ku80 RNA expression levels in a different ovarian cancer miRNA dataset. miR-622 expression levels were statistically significantly inversely correlated with Ku80 RNA expression levels ($p = 0.05$) in a different ovarian cancer dataset.

MREs in Ku70 and Ku80 (Figure 3F). Together, these results suggest that miR-622 regulates the expression of the Ku complex by direct interaction with Ku70 and Ku80 transcripts.

## miR-622 Causes Resistance to PARP Inhibitor and Cisplatin by Downregulating Expression of the Ku Proteins

We examined the impact of Ku downregulation (using small interfering RNAs [siRNAs]) or inhibition (dominant-negative Ku; He et al., 2007) on olaparib and cisplatin sensitivity in parallel with miR-622 overexpression in UWB1.289 cells (Figure 4A) and in *Brca1*$^{-/-}$ MEFs (Figure 4B). We observe that depletion/inhibition (efficacy of siRNAs shown in Figure S4) of the Ku complex and overexpression of miR-622 have a comparable effect on de-sensitizing *BRCA1*-deficient cells to both olaparib and cisplatin. To determine whether the effect of miR-622 on olaparib and cisplatin sensitivity was indeed mediated by Ku suppression, we utilized mouse Ku70 cDNA and rat Ku80 cDNA that lack miR-622 MREs. Next, UWB1.289 cells were co-transfected with miR-622 and mouse Ku70 cDNA or rat Ku80 cDNA. The Ku expression constructs lacking the miR-622 MREs rescued the expression of these genes in the presence of miR-622 mimic, further validating the predicted MREs (Figure 4C, right). Furthermore, individual

expression of the Ku proteins partially rescued the impact of miR-622 on olaparib and cisplatin sensitivity (Figure 4C, left panel).

Ku80 protein and mRNA expression levels are available in primary EOCs in the ovarian TCGA and were correlated with miR-622 expression. Consistent with our results, there is statistically significant inverse correlation of miR-622 with both Ku80 protein and mRNA expression in *BRCA*-inactivated EOCs from the TCGA dataset. Specifically, among the 89 EOCs with either *BRCA1* mutations (n = 38) or *BRCA1* promoter hypermethylation (n = 51), miR-622 expression levels were statistically significantly inversely correlated with Ku80 RNA expression levels ($p = 0.019$) and Ku80 protein levels ($p = 0.029$) as determined by reverse-phase protein array (RPPA) in the TCGA dataset (Figure 4D). This correlation was further confirmed in the independent cohort of EOC patients discussed above; specifically, miR-622 expression levels were statistically significantly inversely correlated with Ku80 RNA expression levels ($p = 0.05$) (Figure 4E). There was no Ku80 protein expression data in that dataset.

### Physiological Relevance of miR-622-Mediated Suppression of the Ku Complex

To explore the physiological relevance of the interactions of miR-622 with Ku70 and Ku80 transcripts, we assessed their expression during the cell cycle, specifically during the G1 to S transition. When synchronizing UWB1.289 cells (profiles shown in Figure S5A), we observe that mRNA levels of Ku70 and Ku80 are reduced in S phase relative to G1 phase (Figure 5A). Interestingly, miR-622 inversely correlates with Ku70 and Ku80 transcripts and is significantly upregulated as cells move into S phase. Antagonizing miR-622 induces a specific increase in Ku70 and Ku80 transcripts (Figure 5B) in S phase. To further confirm the cell-cycle phase specificity of this phenotype while avoiding the artifacts of synchronization, and in a diploid cell line with relatively few genomic abnormalities, we utilized the Fucci system (Sakaue-Sawano et al., 2008) to visualize G1 phase (mKO2-CDT1-RFP) and S phase (Geminin-GFP) in hTERT-immortalized retinal pigment epithelial cell line (RPE-1) cells. The G1 cells and S/G2 phases were separated and isolated using fluorescence-activated cell sorting (FACS) selection. Consistent with the previous results, miR-622 expression inversely correlated with the Ku70 and Ku80 transcripts (Figure 5C) and inhibition of miR-622 in RPE-1 caused a significant increase in Ku70 and Ku80 transcripts in S phase (Figure 5D). To further elucidate the cell-cycle-based impact of miR-622 on the Ku proteins, we utilized luciferase assays (as in Figure 3). We confirmed that antagonizing endogenous miR-622 in S phase significantly increases luciferase activity of constructs with miR-622 recognition elements in the Ku70 and Ku80 transcripts, and this was negated by point mutations that disrupt base pairing between miR-622 and their corresponding binding sites in these transcripts (Figure S5B).

Recruitment of the MRN (Mre11-Rad50-Nbs1) complex is the first step in HR. From a functional standpoint, there is a competitive interplay between the Ku complex and the MRN complex (Balestrini et al., 2013; Foster et al., 2011). Specifically, the overexpression of Ku proteins reduces recruitment of Mre11 to DSBs in S/G2 phase when HR is the preferred DSB repair pathway (Clerici et al., 2008). Therefore, we examined the Mre11 foci during S phase in irradiated cells transfected with miR-622 antagomirs. Consistent with increased Ku levels, antagonizing miR-622 causes a significant decrease in Mre11 foci (Figure 5E). Furthermore, the subsequent step in HR, which is the resection of broken DNA ends and RPA2 foci formation, is also reduced by antagonizing miR-622 (Figure 5F). Importantly, antagonizing miR-622 does not impact the ionizing radiation (IR)-induced generation of DSBs (monitored by $\gamma$-H2AX; Figures 5E and 5G). Together, these results strongly suggest that miR-622 plays a role in the optimal expression of the Ku complex during the cell cycle and potentially facilitates the initiation of HR-mediated DSB repair in S phase.

## DISCUSSION

There is tight regulation of the DSB repair pathways during the cell cycle as HR is restricted to S/G2 phase and NHEJ is predominant in G1 but has moderate activity throughout the cell cycle. Importantly, the choice of DSB repair pathways during the cell cycle is critical for maintaining genomic stability. A decisive factor in this choice is the competition between DNA end protection (which is necessary for NHEJ) and DNA end resection (which is necessary for HR). Depletion of end-protecting factors (such as 53BP1) allows DNA end resection in G1 phase, thereby impairing NHEJ and causing genomic instability (Helmink et al., 2011; Escribano-Diaz et al., 2013). Conversely, ectopic expression of *BRCA1* in G1 phase via the inhibition/deletion of miRNAs suppressing *BRCA1* also allows DSB end resection, leading to unrepaired DSBs (Choi et al., 2014; Dimitrov et al., 2013). During the S/G2 phase of the cell cycle, the relatively error-free HR pathway is preferred, and NHEJ needs to be restricted. The mechanism via which the NHEJ pathway is restricted in S phase remains unknown. Here, we uncover regulation of this step by miR-622. We find that miR-622 plays an important role in maintaining the balance between HR and NHEJ repair pathways during the cell cycle by regulating optimal expression of the Ku complex. The Ku complex is pivotal in pathway choice, as it competes with the MRN complex to capture broken DSB ends and divert it toward the C-NHEJ pathway. miR-622 suppresses NHEJ through targeting of the Ku complex during S phase and enhances initiation of HR-mediated DSB repair in S phase by facilitating the recruitment of Mre11. Therefore, ectopic overexpression of miR-622 can limit NHEJ and boost the HR pathway.

Another important finding of our study is that this role for miR-622 in maintaining a balance between DSB repair pathways may mediate resistance to PARPis and platinum agents in *BRCA1*-inactivated tumors. Elucidating mechanisms of platinum and PARPi resistance in *BRCA*-deficient EOCs is critical in order to identify approaches that suppress de novo and emerging resistant clones. Pharmacological effects that alter the cellular response to PARPis, including increased expression of ABC transporters such as the P-glycoprotein (PgP) efflux

OPEN ACCESS
CellPress

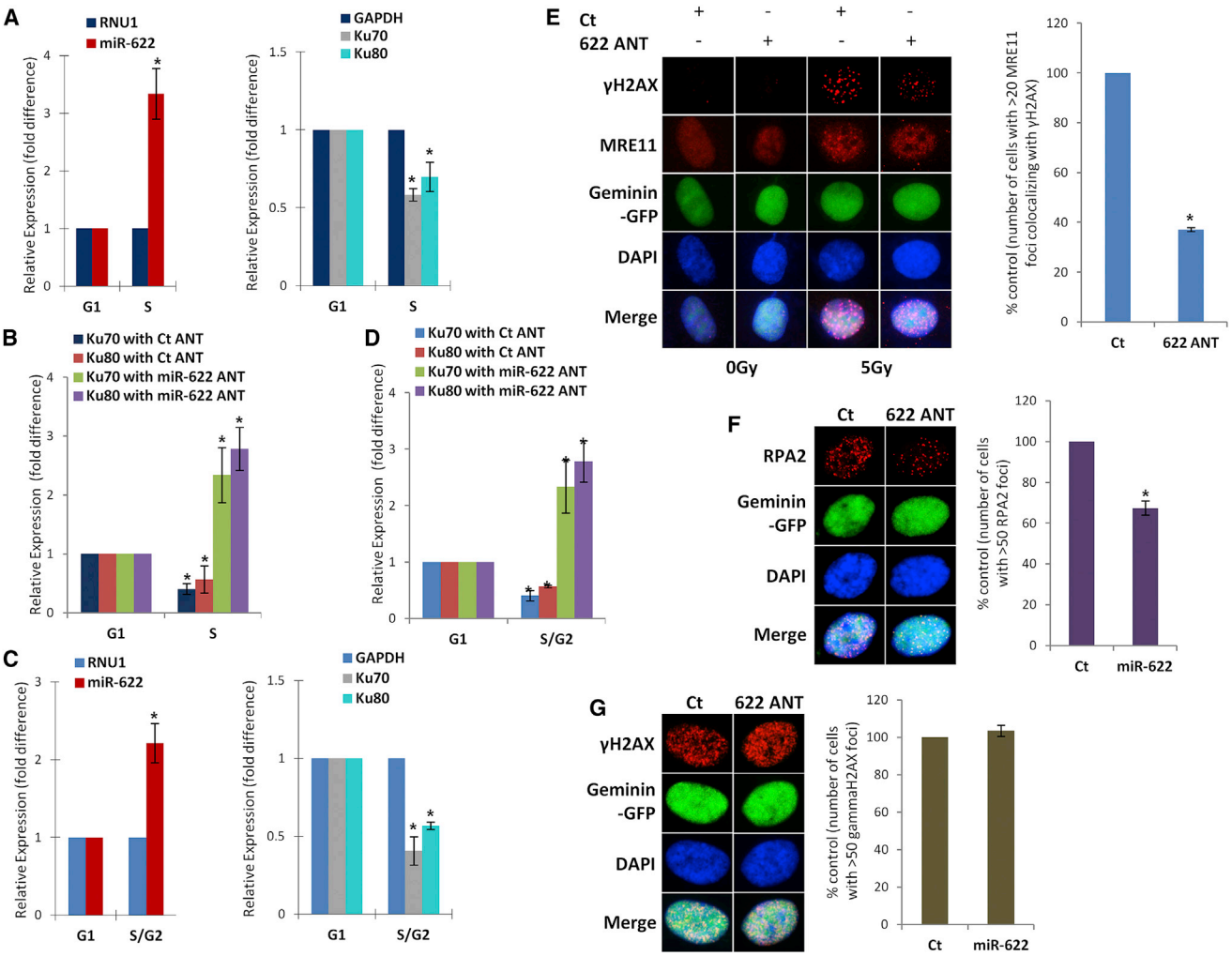


**Figure 5. Impact of miR-622 on DSB Repair during the Cell Cycle**

(A–D) Expression of miRNA and target transcripts in synchronized cells. (A) UWB1.289 cells were synchronized with mimosine, and the relative amount of miR-622 or target mRNA for G1 or S phase was determined by real-time qPCR (normalized to RNU1). (B) UWB1.289 cells were transfected with control ANT or miR-622 ANT and subsequently synchronized with mimosine. Expression of target mRNA was assessed by real-time qPCR in G1 and S phases (normalized to GAPDH). (C) RPE1 Fucci cells were sorted according to cell-cycle-based fluorophore expression, and the relative amount of miR-622 or target mRNA for G1 or S phase was quantified by real-time qPCR. (D) RPE1 Fucci cells were transfected with control ANT or miR-622 ANT and sorted for the cell cycle. Expression of target mRNA was assessed by real-time qPCR in G1 and S phases. Mean ± SD of three independent experiments is shown, and statistical significance is indicated by $^*p < 0.05$.

(E–G) Impact of miR-622 inhibition on recruitment of DSB proteins. RPE1 Fucci cells were transfected with control ANT or miR-622 ANT and irradiated with 5 Gy IR (for γH2AX and Mre11, 3 hr after IR) or 10 Gy (for RPA2, 4 hr after IR). Cells were stained for Mre11 (red) (E), RPA2 (red), (F) or γH2AX (red) (G) and 4′,6-diamidino-2-phenylindole (blue). The images were captured by fluorescence microscopy, and Mre11, RPA2, or γH2AX focus-positive cells (with >20 foci or >50 foci) at S phase (green) were quantified by comparing 100 cells.

pump, have been associated with PARPi resistance in *BRCA1*-mutated breast and ovarian cancer, but their clinical relevance for platinum resistance remains unclear. Furthermore, although a number of resistance mechanisms have been described (Konstantinopoulos et al., 2015), only secondary *BRCA1/2* mutations restoring BRCA1/2 protein functionality have been validated in multiple EOC patient cohorts. It is noteworthy that most of these models systems have not investigated ovarian carcinomas, thereby undermining their clinical relevance. In this regard, our study highlights a mechanism of PARPi resistance in *BRCA1*-deficient EOC patients involving miR-622 overexpression and represents an extension of its physiological role in maintaining the balance of DSB repair pathways.

Importantly, unlike 53BP1 loss, which confers only PARPi resistance, this resistance mechanism confers resistance to both platinum and PARPis. Although miRNA expression has been recently implicated in mediating HR deficiency and response to platinum and PARPis (Liu et al., 2015), we implicate a miRNA in doing exactly the opposite, i.e., mediating PARPi and platinum resistance by rescuing HR deficiency.

Strikingly, the clinical relevance of this resistance mechanism was evident in two different ovarian cancer datasets whereby overexpression of miR-622 was associated with an inferior outcome after platinum chemotherapy in *BRCA1*-inactivated tumors. Of note, the expression of miR-622 was also inversely correlated with protein and mRNA expression levels of Ku80, thereby clinically validating our experimental observations that the association of miR-622 with worse outcome may indeed be related to its targeting of the Ku complex. In conclusion, our work suggests a role for miR-622 in regulating the balance between HR and NHEJ in the cell cycle and highlights a potential role of this miRNA as a biomarker of responsiveness to platinum and PARPis in *BRCA1*-inactivated EOCs. Furthermore, miR-622 may be a promising target for augmenting PARPi and platinum response in *BRCA1*-inactivated EOCs.

## EXPERIMENTAL PROCEDURES

### Viability Assay

Viability assays were done as previously described (Choi et al., 2014).

### Ovarian Cancer Datasets and Statistical Analysis

The association between miR-622 expression levels and outcome (OS and DFS) was assessed in two clinically annotated ovarian cancer datasets with miRNA expression data. First, we accessed expression data from the ovarian TCGA dataset, which included 38 tumors with *BRCA1*-mutations (out of 316 EOCs that underwent whole-exome sequencing) and 51 tumors (out of 489 tumors with DNA promoter methylation data) with *BRCA1* epigenetic silencing via promoter hypermethylation. Promoter hypermethylation was assessed using the same criteria described in the ovarian TCGA dataset publication. The second dataset included expression data from 60 patients with newly diagnosed FIGO stage III or IV tumors, all with serous histology (Shih et al., 2011). The t test and Fisher's exact test were used to analyze the clinical and experimental data. The correlation between miR-622 and Ku80 expression levels was assessed using the Pearson's correlation coefficient. Significance was defined as a $p < 0.05$; all reported p values are two sided. OS and DFS curves were generated using the Kaplan-Meier method, and statistical significance was assessed using the log-rank test.

### Non-homologous End-Joining Reporter Assay

NHEJ reporter assays were done as the HR assays previously described. (Choi et al., 2014) by using U2OS cells carrying a single copy of the recombination substrate with two tandem I-SceI sites.

### Chromosome Breakage Analysis

*Brca1*$^{-/-}$ MEF cells were transfected with indicated miRNA mimics for 24 hr followed by treatment with or without the indicated concentrations of PARPi (olaparib) for 24, 48, or 72 hr. Cells were exposed to 100 ng/ml Colcemid for 2 hr followed by treatment with a hypotonic solution (0.075 M KCl) for 20 min and fixed with 3:1 methanol/acetic acid solution. Slides were stained with Wright's stain, and $\geq$50 metaphase spreads were scored for aberrations.

### Immunofluorescence

Immunofluorescence in UWB1.289 and RPE1 Fucci cells was done as previously described (Lee et al., 2010) using RAD51 (Santa Cruz Biotechnology #sc-8349), $\gamma$-H2AX (Cell Signaling #9718S), RPA2 (Abcam #ab2175), and Mre11 (Novus Biologicals #NB100-142)

### RNA Isolation and Real-Time qPCR

Total RNA was prepared and expression was analyzed by real-time qPCR as described previously (Moskwa et al., 2011).

Gene-specific primers used for real-time qPCR are as follows:

53BP1-F-1, 5′-GTCATTGAGCAGTTACCTCAG-3′; R-1, GGGAATGTGTAGTATTGCCTG
53BP1-F-2, 5′-ATGGTGGAGACCCATGATCC-3′; R-2, GTCTTCTGGGGACTGGCAAC
KU70-F-1, 5′-GTTGATGCCTCCAAGGCTATG-3′; R-2, GCACCTGGATTATCCAGCTC
KU70-F-2, 5′-AATTCAGGTGACTCCTCCAG-3′; R-2, TGAAGTGCTGCTGCAGCAC
KU80-F-1, 5′-AAGCAAAATCCAACCAGGTTCT-3′; R-1, GAATTGCAGGGAGATGTCACA
KU80-F-2, 5′-ACTCTGATCACCAAAGAGGAA-3′; R-2, TGGCAGCTCTCTTAGATTCC
APTX-F, 5′-TGGAAGCAGTTGTGATTGGG-3′; R, CACCATGTGGAGAACCTGG
APLF-F, 5′-GAAGCCAAATCTATGGTGCTA-3′; R, CTTCATCAAGCACTTGACTGT.

### Immunoblots

Immunoblots were done as described previously (Lee et al., 2010; Moskwa et al., 2011) with 53BP1 (Cell Signaling Technology #4937), Ku70 (Santa Cruz #sc-1486), Ku80 (Thermo Scientific #PA5-17454), and $\alpha$-tubulin (Sigma #T5168) antibodies.

### Immunoprecipitation of miRNA Targets

Immunoprecipitation of miRNA target with biotinylated miR-622 was done with UWB1.289 cells as previously described (Choi et al., 2014).

### Luciferase Assay

The wild-type (WT) or mutant (Mt) MREs of target genes were synthesized as oligonucleotide sequences and annealed and cloned in psiCHECK2 (Promega) downstream to *Renilla* luciferase. Luciferase assay in UWB1.289 cells using WT and Mt MRE constructs was done as described previously (Moskwa et al., 2011). The oligonucleotide sequences are as follows:

KU70-MRE1 forward (F), 5′-TCGAAAGCAATGAATAAAAGACTGGGAAGAAGCAATGAATAAAAGACTGG-3′; reverse (R), 5′-GGCCCCAGTCTTTTATTCATTGCTTCTTCCCAGTCTTTTATTCATTGCTT; KU70-MRE2-F, 5′-TCGAACCAAGCACTTCCAGGACTGAGAAGACCAAGCACTTCCAGGACTGA-3′; R, 5′-GGCCTCAGTCCTGGAAGTGCTTGGTCTTCTCAGTCCTGGAAGTGCTTGGT-3′; KU70-MRE1+2-F, 5′-TCGAAAGCAATGAATAAAAGACTGGGAAGACCAAGCACTTCCAGGACTGA-3′; R, 5′-GGCCTCAGTCCTGGAAGTGCTTGGTCTTCCCAGTCTTTTATTCATTGCTT-3′; KU80-MRE1-F, 5′-TCGAAGCTAAAAAATTAAAGACTGAGAAGAGCTAAAAAATTAAAGACTGA-3′; R, 5′-GGCCTCAGTCTTTAATTTTTTAGCTCTTCTCAGTCTTTAATTTTTTAGCT-3′; KU80-MRE2-F, 5′-TCGATTTATGAAGAGCATAGACTGCGAAGTTTATGAAGAGCATAGACTGC-3′; R, 5′-GGCCGCAGTCTATGCTCTTCATAAACTTCGCAGTCTATGCTCTTCATAAA-3′; KU80-MRE1+2-F, R, 5′-GGCCGCAGTCTATGCTCTTCATAAACTTCTCAGTCTTTAATTTTTTAGCT-3′.

The oligonucleotides for mutant MREs are as follows:

Mt KU70-MRE1+2-F, 5′-TCGAAAGGTTGGAATAAATCTGACGGAAGAGGTAGCTGGAGCATCTGACA-3′; R, 5′-GGCCTGTCAGATGCTCCAGCTACCTCTTCCGTCAGATTTATTCCAACCTT-3′; Mt KU80-MRE1+2-F, 5′-TCGAACGAAATTAAAGTATCTGACAGAAGTTTATGAAGTCGATTCTGACC-3′; R, 5′-GGCCGGTCAGAATCGACTTCATAAACTTCTGTCAGATACTTTAATTTCGT-3′.

### Cell-Cycle Synchronization and Sorting

Cell synchronization was performed in UWB1.289 cells as previously described (Choi et al., 2014). Cells transfected with miR-622 antagomir with rat Ku70 or mouse Ku80 cDNA (a gift from Andre Nussenzweig at the National Cancer Institute) were similarly synchronized 48 hr after transfection. RPE1

Fucci cells were sorted using BD FACSAria based on fluorophore expression according to the cell cycle (RFP, G1 phase; GFP, S/G2/M phase).

### miRNA Target Prediction

We used a candidate-based prediction approach by using PITA (http://genie.weizmann.ac.il/pubs/mir07/mir07_data.html) to analyze the Human DNA Repair Gene list (http://sciencepark.mdanderson.org/labs/wood/dna_repair_genes.html#Human%20DNA%20Repair%20Genes), which resulted in a list of DNA damage response genes predicted as targets of miRNAs of our interest. Predicted targets are listed in Figure S2 and further validated as explained in this article.

## SUPPLEMENTAL INFORMATION

Supplemental Information includes five figures and can be found with this article online at http://dx.doi.org/10.1016/j.celrep.2015.12.046.

## ACKNOWLEDGMENTS

D.C. is supported by grants R01 AI101897-01 (NIAID) and R01CA142698-07 (NCI), a Basic Scholar Grant (American Cancer Society), a Leukemia and Lymphoma Society Scholar Grant, the Claudia Adams Barr Program for Innovative Cancer Research, a Breast SPORE Pilot Award, the Robert and Deborah First Fund, and the Mary Kay Foundation. P.A.K. is supported by the Susan Smith Center for Women's Cancers and a Department of Defense Ovarian Cancer Academy Award (W81XWH-10-1-0585). The *Brca1*$^{-/-}$ MEFs were a gift from Andre Nussenzweig, and NHEJ reporter construct was a gift from Jeremy Stark.

Received: September 28, 2015
Revised: November 19, 2015
Accepted: December 4, 2015
Published: January 7, 2016

## REFERENCES

Balestrini, A., Ristic, D., Dionne, I., Liu, X.Z., Wyman, C., Wellinger, R.J., and Petrini, J.H. (2013). The Ku heterodimer and the metabolism of single-ended DNA double-strand breaks. Cell Rep. *3*, 2033–2045.

Bennardo, N., Cheng, A., Huang, N., and Stark, J.M. (2008). Alternative-NHEJ is a mechanistically distinct pathway of mammalian chromosome break repair. PLoS Genet. *4*, e1000110.

Boersma, V., Moatti, N., Segura-Bayona, S., Peuscher, M.H., van der Torre, J., Wevers, B.A., Orthwein, A., Durocher, D., and Jacobs, J.J. (2015). MAD2L2 controls DNA repair at telomeres and DNA breaks by inhibiting 5′ end resection. Nature *521*, 537–540.

Bouwman, P., Aly, A., Escandell, J.M., Pieterse, M., Bartkova, J., van der Gulden, H., Hiddingh, S., Thanasoula, M., Kulkarni, A., Yang, Q., et al. (2010). 53BP1 loss rescues BRCA1 deficiency and is associated with triple-negative and BRCA-mutated breast cancers. Nat. Struct. Mol. Biol. *17*, 688–695.

Bunting, S.F., Callén, E., Wong, N., Chen, H.T., Polato, F., Gunn, A., Bothmer, A., Feldhahn, N., Fernandez-Capetillo, O., Cao, L., et al. (2010). 53BP1 inhibits homologous recombination in Brca1-deficient cells by blocking resection of DNA breaks. Cell *141*, 243–254.

Bunting, S.F., Callén, E., Kozak, M.L., Kim, J.M., Wong, N., López-Contreras, A.J., Ludwig, T., Baer, R., Faryabi, R.B., Malhowski, A., et al. (2012). BRCA1 functions independently of homologous recombination in DNA interstrand crosslink repair. Mol. Cell *46*, 125–135.

TCGA (The Cancer Genome Atlas Research Network) (2011). Integrated genomic analyses of ovarian carcinoma. Nature *474*, 609–615.

Chapman, J.R., Sossick, A.J., Boulton, S.J., and Jackson, S.P. (2012a). BRCA1-associated exclusion of 53BP1 from DNA damage sites underlies temporal control of DNA repair. J. Cell Sci. *125*, 3529–3534.

Chapman, J.R., Taylor, M.R., and Boulton, S.J. (2012b). Playing the end game: DNA double-strand break repair pathway choice. Mol. Cell *47*, 497–510.

Choi, Y.E., Pan, Y., Park, E., Konstantinopoulos, P., De, S., D'Andrea, A., and Chowdhury, D. (2014). MicroRNAs down-regulate homologous recombination in the G1 phase of cycling cells to maintain genomic stability. eLife *3*, e02445.

Ciccia, A., and Elledge, S.J. (2010). The DNA damage response: making it safe to play with knives. Mol. Cell *40*, 179–204.

Clerici, M., Mantiero, D., Guerini, I., Lucchini, G., and Longhese, M.P. (2008). The Yku70-Yku80 complex contributes to regulate double-strand break processing and checkpoint activation during the cell cycle. EMBO Rep. *9*, 810–818.

Deriano, L., and Roth, D.B. (2013). Modernizing the nonhomologous end-joining repertoire: alternative and classical NHEJ share the stage. Annu. Rev. Genet. *47*, 433–455.

Dimitrov, S.D., Lu, D., Naetar, N., Hu, Y., Pathania, S., Kanellopoulou, C., and Livingston, D.M. (2013). Physiological modulation of endogenous BRCA1 p220 abundance suppresses DNA damage during the cell cycle. Genes Dev. *27*, 2274–2291.

Escribano-Diaz, C., Orthwein, A., Fradet-Turcotte, A., Xing, M., Young, J.T., Tkac, J., Cook, M.A., Rosebrock, A.P., Munro, M., Canny, M.D., et al. (2013). A cell cycle-dependent regulatory circuit composed of 53BP1-RIF1 and BRCA1-CtIP controls DNA repair pathway choice. Mol. Cell. *9*, 872–883.

Fattah, F., Lee, E.H., Weisensel, N., Wang, Y., Lichter, N., and Hendrickson, E.A. (2010). Ku regulates the non-homologous end joining pathway choice of DNA double-strand break repair in human somatic cells. PLoS Genet. *6*, e1000855.

Fong, P.C., Boss, D.S., Yap, T.A., Tutt, A., Wu, P., Mergui-Roelvink, M., Mortimer, P., Swaisland, H., Lau, A., O'Connor, M.J., et al. (2009). Inhibition of poly(ADP-ribose) polymerase in tumors from BRCA mutation carriers. N. Engl. J. Med. *361*, 123–134.

Foster, S.S., Balestrini, A., and Petrini, J.H. (2011). Functional interplay of the Mre11 nuclease and Ku in the response to replication-associated DNA damage. Mol. Cell. Biol. *31*, 4379–4389.

He, F., Li, L., Kim, D., Wen, B., Deng, X., Gutin, P.H., Ling, C.C., and Li, G.C. (2007). Adenovirus-mediated expression of a dominant negative Ku70 fragment radiosensitizes human tumor cells under aerobic and hypoxic conditions. Cancer Res. *67*, 634–642.

Helmink, B.A., Tubbs, A.T., Dorsett, Y., Bednarski, J.J., Walker, L.M., Feng, Z., Sharma, G.G., McKinnon, P.J., Zhang, J., Bassing, C.H., and Sleckman, B.P. (2011). H2AX prevents CtIP-mediated DNA end resection and aberrant repair in G1-phase lymphocytes. Nature *469*, 245–249.

Konstantinopoulos, P.A., Ceccaldi, R., Shapiro, G.I., and D'Andrea, A.D. (2015). Homologous recombination deficiency: exploiting the fundamental vulnerability of ovarian cancer. Cancer Discov. *5*, 1137–1154.

Lal, A., Navarro, F., Maher, C.A., Maliszewski, L.E., Yan, N., O'Day, E., Chowdhury, D., Dykxhoorn, D.M., Tsai, P., Hofmann, O., et al. (2009). miR-24 Inhibits cell proliferation by targeting E2F2, MYC, and other cell-cycle genes via binding to "seedless" 3'UTR microRNA recognition elements. Mol. Cell *35*, 610–625.

Lal, A., Thomas, M.P., Altschuler, G., Navarro, F., O'Day, E., Li, X.L., Concepcion, C., Han, Y.C., Thiery, J., Rajani, D.K., et al. (2011). Capture of microRNA-bound mRNAs identifies the tumor suppressor miR-34a as a regulator of growth factor signaling. PLoS Genet. *7*, e1002363.

Lee, D.H., Pan, Y., Kanner, S., Sung, P., Borowiec, J.A., and Chowdhury, D. (2010). A PP4 phosphatase complex dephosphorylates RPA2 to facilitate DNA repair via homologous recombination. Nat. Struct. Mol. Biol. *17*, 365–372.

Liu, G., Yang, D., Rupaimoole, R., Pecot, C.V., Sun, Y., Mangala, L.S., Li, X., Ji, P., Cogdell, D., Hu, L., et al. (2015). Augmentation of response to chemotherapy by microRNA-506 through regulation of RAD51 in serous ovarian cancers. J. Natl. Cancer Inst. *107*, djv108.

Moskwa, P., Buffa, F.M., Pan, Y., Panchakshari, R., Gottipati, P., Muschel, R.J., Beech, J., Kulshrestha, R., Abdelmohsen, K., Weinstock, D.M., et al. (2011). miR-182-mediated downregulation of BRCA1 impacts DNA repair and sensitivity to PARP inhibitors. Mol. Cell *41*, 210–220.

Norquist, B., Wurz, K.A., Pennil, C.C., Garcia, R., Gross, J., Sakai, W., Karlan, B.Y., Taniguchi, T., and Swisher, E.M. (2011). Secondary somatic mutations restoring BRCA1/2 predict chemotherapy resistance in hereditary ovarian carcinomas. J. Clin. Oncol. *29*, 3008–3015.

Orom, U.A., and Lund, A.H. (2007). Isolation of microRNA targets using biotinylated synthetic microRNAs. Methods *43*, 162–165.

Sakaue-Sawano, A., Kurokawa, H., Morimura, T., Hanyu, A., Hama, H., Osawa, H., Kashiwagi, S., Fukami, K., Miyata, T., Miyoshi, H., et al. (2008). Visualizing spatiotemporal dynamics of multicellular cell-cycle progression. Cell *132*, 487–498.

Shih, K.K., Qin, L.X., Tanner, E.J., Zhou, Q., Bisogna, M., Dao, F., Olvera, N., Viale, A., Barakat, R.R., and Levine, D.A. (2011). A microRNA survival signature (MiSS) for advanced ovarian cancer. Gynecol. Oncol. *121*, 444–450.

Xu, G., Chapman, J.R., Brandsma, I., Yuan, J., Mistrik, M., Bouwman, P., Bartkova, J., Gogola, E., Warmerdam, D., Barazas, M., et al. (2015). REV7 counteracts DNA double-strand break resection and affects PARP inhibition. Nature *521*, 541–544.